

# Water Sludge Drying: Modelling of a Solar Thermal Plant for a Solar Vacuum Dryer

Ruben Bartali<sup>1</sup>, Özgür Bayer<sup>2</sup>, Deniz Pınarlı<sup>2</sup>, Selin Erdoğan<sup>2</sup>, Michele Bolognese<sup>1</sup>, Derek Baker<sup>2</sup>, Luca Praticò<sup>1,3</sup> and Luigi Crema<sup>1</sup>

<sup>1</sup> Fondazione Bruno Kessler, Applied Research on Energy System Unit, Via Sommarive, 18, 38123, Trento, Italy

<sup>2</sup> Middle East Technical University, Mechanical Engineering Department, 06800, Ankara, Turkey

<sup>3</sup> "Sapienza" University of Rome, Via Eudossiana 18, Rome, Italy

The use of dryers that operate at pressures below atmospheric can be a smart technological solution to allow better matching between commercial solar collectors and solar drying applications. At atmospheric pressure, water boils at 100°C, while at 500 mbar, 200 mbar, and 100 mbar water boils at 81.5°C, 60.5°C, and 45.6 °C, respectively. For instance, for Evacuated Tube Collectors (ETC) it is challenging to provide a constant heat at temperatures higher than 90°C. Furthermore, the tuning of the boiling temperature allows a better adaptation of the solar heat provided by a solar plant to the heat required for water sludge drying. To understand the technical feasibility of a Vacuum Solar dryer for water sludge, two solar plants with two types of solar collectors with water as the working fluid were modelled: i) ETC ii) parabolic trough collector (PTC). The modelling and design of a vacuum dryer for the drying of water sludges is presented. The results reveal that a light vacuum can improve the performance in terms of the solar fraction of the solar dryer for both ETC and PTC solar fields.

*Keywords: ETC, PTC, solar vacuum dryer, predictive simulation tools, decarbonization*

---

## 1. Introduction

Solar-thermal driven dryers (i.e. *solar dryers*) are a potentially attractive technology for a wide range of industrial sectors including chemical, food and beverage, plastic, and metallurgical (Hisan *et al.*, no date). Until 2018, approximately 75% of solar dryer articles published in the literature are dedicated to the agro-food sector (e.g. drying of fruit and vegetables), while the other articles are mainly devoted to drying processes for timber and other forest products, water waste, heat pumps, carpet production, and natural rubber (Goh *et al.*, 2011)(Bekkioui *et al.*, 2011) (Fuller, 2002)(Bal, Satya and Naik, 2010). One key parameter when assessing the feasibility for powering an industrial drying process using solar thermal is the temperature required by the drying processes (Hisan *et al.*, no date). The temperature of the drying process allows the proper choice of solar collector, the heat transfer fluid (HTF), and heat exchanger. In the agro-food sector, solar dryers are widely used because the temperatures required for drying processes are typically relatively low (e.g. 40-70°C) and easy to reach using commercially-available, inexpensive and efficient collectors such as flat-plate liquid collectors, air collectors, and greenhouses. Drying cabinets typically work in the temperature range of 60°C to 80°C, and usually, in this range, the use of an evacuated tube collector with water as the heat transfer fluid is the appropriate choice (Prakash and Kumar, 2014). On the other hand, for applications such as paper drying, and drying a finished product, the temperature required is often higher than 100°C or 200°C and the collector used in this kind of application can be a parabolic trough collector (PTC) or evacuated flat plate collector. Moreover, in this range of temperature, pressurized water and thermal oil are typical heat transfer fluids.

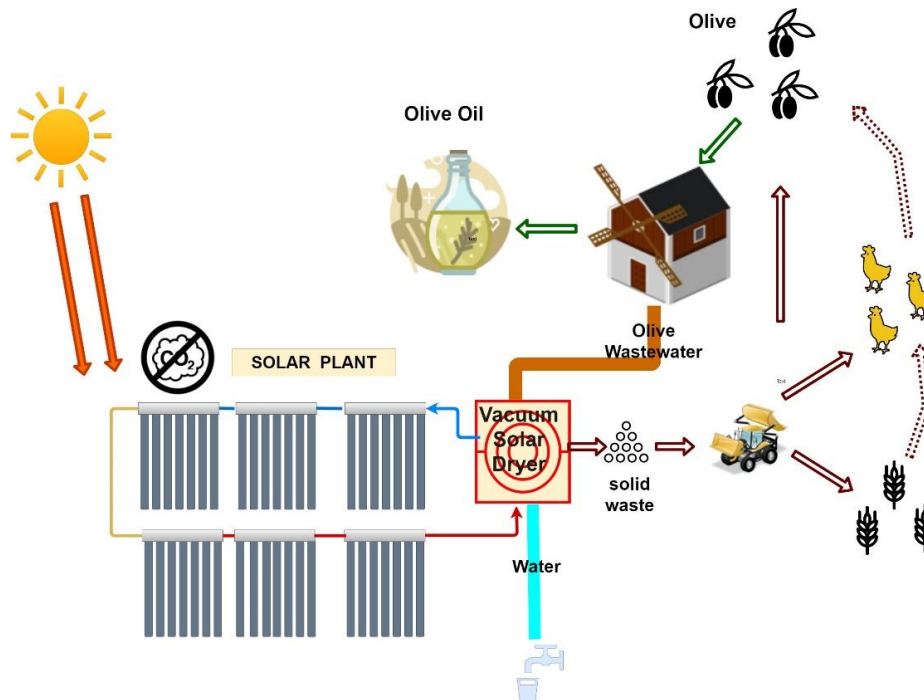


Fig. 1. Sketch of a solar plant for solar drying of Olive water sludge, the solid waste can be also valorized in other agro-food cycles (Dermeche *et al.*, 2013)(Encinar *et al.*, 2008) .

One of the most attractive emerging sectors for solar drying is waste water treatment, such as pharmaceutical wastewater. Another interesting application is the drying of microalgae used for instance in biofuel production (Gouveia *et al.*, 2016)(Villagrancia *et al.*, 2016). In all these applications to promote the use of solar energies, it is very important to provide in an efficient mode the heat from the solar field to the dryer. Vacuum technologies can be useful to optimize the performances of the solar collector in the solar drying sector. Water, in fact, boils at 100°C at atmospheric pressure, but the reduction of pressure decreases the boiling temperature and can be a smart technological solution to allow the thermal matching of commercial solar collectors with solar drying applications. For instance, for Evacuated Tube Collectors (ETCs) providing a constant heat at temperatures higher than 90° is challenging, while using Parabolic Trough Collectors (PTCs) maintaining temperatures higher than 100°C is much easier. But the PTC technology requires sophisticated optics, a tracking system, and the installation is more complex. Therefore, to amortize the investment it is very important to maximize the use of the heat provided by the solar field. For this reason, in this work, we study the solar field with a vacuum dryer system used to treat olive water sludge (Wu *et al.*, 2010) (Bennamoun, 2012). A schematic of the overall system is presented in Fig. 1. In this work, a solar dryer with a maximum power of 280 kW has been analyzed. The solar dryer under study uses vacuum technology to reduce the boiling temperature of the water sludge to be dried. Two solar plants with two different solar collector models were modelled, to understand the benefits of a solar dryer.

- Vacuum Solar dryer with ETC and water as the HTF;
- Vacuum Solar dryer with PTC and water as the HTF.

For both simulations, we considered a common vacuum solar dryer. In the first part of this work, the design of the solar vacuum dryer and solar field is reported. In the second part, the modelling results obtained for the ETC and PTC solar fields are reported and compared.

## 2. Methods

### 2.1 Design of the Vacuum solar Dryer

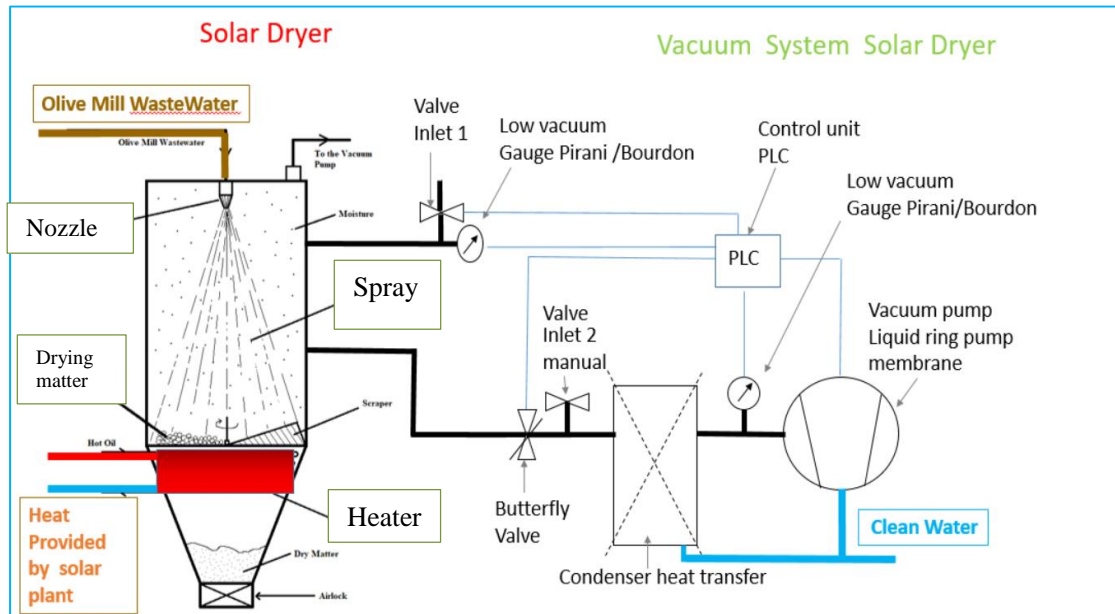


Fig. 2 Design of solar dryer with the vacuum system

The design of the solar vacuum dryer is depicted Fig. 2, and it is composed of a vacuum chamber and a vacuum system. The vacuum system design contains a pumped line and a venting (inlet) line. For this kind of vacuum Pirani or Bourdon sensors can be used, and the vacuum pumping speed (that allows the control of the vacuum pressure in the dryer) can be controlled by a butterfly valve. The vacuum can be generated using a liquid ring vacuum pump or a membrane pump. The vacuum system can be controlled by the Programmable Logic Controller (PLC). One of the most critical techno-economical parameters in the design of a vacuum system is the thickness of the wall of the vacuum chamber; if the wall is too thin, the external pressure will deform the dryer apparatus (collapse) and if the thickness is too thick, the weight and the cost of the apparatus can be too high. The thickness of the wall strongly depends on the volume of the vacuum tank. The volume of the tank has been dimensioned to ensure on the one hand the complete evaporation of the liquid and on the other hand to avoid a deformation induced by external pressure. Droplet diameter size coming out of the spray dryer was assumed as 1 mm and required vacancy around the droplet was found as 5 times of droplet size. Considering: i) the amount of wastewater that should be dried per second, ii) droplet speed and vacancy to droplet ratio, and iii) the structural problem induced by the vacuum (wall thickness), a cylindrical dryer tank with 61 cm diameter and 1-meter height with a spraying angle of 33,9° has been considered. The wall thickness was found as a minimum value of 2 mm with stress and fracture analyses (eq. 1). Aluminium was selected as the tank material and its technical characteristics are presented in Table 1.

Table 1: Technical characteristics of aluminium

Yield stress of aluminium	0.78 MPa
$K_{Ic}$ (Critical Stress Intensity Factor)	24 MPa.m <sup>1/2</sup>
Possible crack size	1mm
Vacuum Pressure	100 mbar

$$\text{Wall Thickness} = (\text{Vacuum Pressure} * \text{Tank Radius}) / (\text{Safety Factor} * \text{Yield Stress}) \quad (\text{eq.1})$$

The vacuum dryer has been designed with a vacuum system which can reach a vacuum pressure of 100 mbar which corresponds to 45.8 °C of water boiling temperature. Using this vacuum pressure, the system presents lower power input need, which was found as 216 kW.

In solar vacuum dryers two strategies can be used to adjust the heat power at the output. The first performs a variation of mass flow rate. The second is obtained through a variation of boiling temperature:

- 1) Arranging vacuum pressure inside the tank so that the boiling temperature of water changes. At 500 mbar, the boiling temperature is 81.5°C whereas at 200 mbar, it is 60.5°C. With higher vacuum, less energy is required to heat up the sprayed mill wastewater to the boiling temperature. It is therefore possible to adjust the pressure according to the availability of solar radiation, during the day, to ensure greater uniformity of thermal energy production.
- 2) Adjusting the mass flow rate of mill wastewater through the spray nozzle. The system is capable of drying more material when the solar energy input is higher.

Based on the average amount of olive processed per year, a daily average production was calculated as 0.83 tons per day. Moreover, the amount of wastewater produced was calculated assuming 5% of wastewater in solid matter and remained part in water (average value). The required flow rate of wastewater is calculated as:

$$\dot{m}_w = \frac{\text{daily wastewater outcome}}{\text{daily PTC working hours}} \quad (\text{eq.2})$$

All these calculations were embedded in Visual Basic (VB) code such that if any of these parameters needs to be changed, new size outputs are provided by a button running with this code.

PARAMETERS		OUTPUTS		
Olive [tones/year]	300	Volume flow rate of mill water (through nozzle) [L/min]	4,675	L/min
Mill water / oil [m <sup>3</sup> /ton]	1	Required Power	196,317	kW
days per year	93	Number of Droplets	186012,340	
Solid Ratio Percentage [%]	5	Minimum volume needed in dryer for the droplet area	0,097	m <sup>3</sup>
Solar Energy Hours (7.00-19.00)	12	Radius of cylindrical design	0,305	m
Density of water	958,35	Spray Angle	33,920	degrees
hfg of water [kJ/kg]	2493	Wall Thickness	1,955	mm
Droplet size [mm]	1			
Droplet speed [m/s]	0,1			
Height of dryer [m]	1			
Vacancy radius/particle radius	5			
Vacuum Pressure [mbar]	200			
Yield Strength [Mpa]	0,78			
Kic of material [Mpa*m <sup>1/2</sup> ]	24			
Safety Factor	4			
Crack length [cm]	1			
Temperature of mill water	25			
Cp of water	4,2199			
Evaporation Temp (Temp inside vacuum)	60,5			

Fig. 3 Picture of VBA interface

The VB routine was designed to model the characteristics of the solar vacuum dryer. The code takes as inputs the constant sludge flow rate of the production line and the vacuum pressure provided by the system. A medium-sized factory that processes 300 tons of olives per year was considered. The total thermal power ( $P$ ) required for the drying process is estimated as Equation 3. Two periods are considered for building Equation 3: the total amount of power needed to bring all of the mill water to the boiling temperature of water for the present vacuum condition and to evaporate the water portion of the whole fluid. :

$$P = \dot{m}_w \cdot c_p \cdot (T_{evap,p} - T_w) + \dot{m}_w \cdot \rho_w \cdot h_{fg} \quad (\text{eq.3})$$

where

$\dot{m}_w$  : Mass flow rate of mill wastewater (or the fluid which will be dried) flowing through nozzle [kg s<sup>-1</sup>]

$c_p$  : Specific heat capacity of mill wastewater [J kg<sup>-1</sup> °C<sup>-1</sup>]

$T_w$  : Temperature of mill wastewater coming from nozzle to the tank [°C]

$T_{evap,p}$  : Evaporation/ boiling temperature of water at provided vacuum pressure [°C]

$\rho_w$  : ratio of water in mill wastewater [mass of water/mass of mill wastewater]

$h_{fg}$  : specific enthalpy of evaporation of water [kJ kg<sup>-1</sup>]

$\dot{m}_w$  correspond to a value of about 0,0745 kg/s when Equation 2 is used with the average amount of olive processed per year for a middle-sized factory consideration. It is the total amount of fluid (mill water) which should be brought to the boiling temperature. After the whole fluid reaches that temperature, only the water portion should be evaporated which corresponds to the  $\dot{m}_w \times \rho_w$  where  $\rho_w$  (the ratio of water in mill water) is

95%.  $T_w$  is the first temperature of mill water before entering the drying cycle and assumed as 25°C.  $T_{evap,p}$ ,  $h_{fg}$  and  $c_p$  values are dependent on the temperature and pressure values inside the tank, therefore changeable. The corresponding values for each temperature and pressure variation are tabulated in a separate Excel sheet and the “VLOOKUP” formulas in “Parameters” table pulls the right value for the inputted vacuum pressure from these tables, then pastes to the related cell in the “Parameters” Table seen in Figure 3. For instance, for a vacuum pressure of 200mbar,  $T_{evap,p}$ ,  $c_p$  and  $h_{fg}$  values are pulled. Pulled values for 200mbar are  $T_{evap,p}=60.5^\circ\text{C}$ ,  $c_p = 4.1816 \text{ kJ/kg K}$  and  $h_{fg} = 2358.5 \text{ kJ/kg}$ . Required power input is 196.317 kW for that case. When the vacuum pressure is increased to 500mbar,  $T_{evap,p}$  becomes 81.5°C, and corresponding values to that temperature are:  $c_p = 4.2199 \text{ kJ/kgK}$  and  $h_{fg} = 2302.3 \text{ kJ/kg}$ . Required power input for that case is 188.400 kW.

## 2.2 Modelling of solar field

Considering the features of the solar dryer described above, the solar field has been modelled employing either the PTC or ETC. The PTC field with north-south axis tracking is connected to a thermal storage unit in which the HTF acts as the storage medium. While the HTF is being circulated through the absorber pipe of PTC by a pump, it absorbs concentrated solar irradiation. The flow in the absorber pipe is considered as uniform, incompressible, single-phase flow with constant properties. A 1-D transient thermal model is employed to obtain the HTF temperature as a function of time and location along the absorber pipe. Neglecting axial conduction, the energy equation is given as follows:

$$\frac{\partial T}{\partial t}(x, t) + u \frac{\partial T}{\partial x}(x, t) = \frac{q_{abs} - q_{loss,col}}{L\rho Ac_p} \quad (\text{eq.4})$$

Where  $u$  is the flow velocity,  $q_{abs}$  is the absorbed solar heat,  $q_{loss}$  is the heat loss to environment from the collector,  $L$  is the collector length,  $\rho$  is the HTF density,  $A$  is the cross-sectional area of receiver pipe and  $c_p$  is the specific heat of the HTF.  $c_p$  is assumed to be constant due to its small variation with temperature. Assuming constant collector efficiency,  $q_{abs}$  is calculated by the following equation:

$$q_{abs} = \eta_0 (GII) A_{aperture} \quad (\text{eq. 5})$$

Where  $\eta_0$  is the average collector efficiency and  $GII$  is the global inclined irradiance. An overall heat transfer coefficient is determined to estimate the convective heat loss to the ambient air. Neglecting radiative losses,  $q_{loss}$  is calculated as follows:

$$q_{loss,col} = U_{col} A_{p,col} (T_{avg,col} - T_{amb}) \quad (\text{eq. 6})$$

The Partial Derivative Equations (PDE), eq. (4), is solved numerically using the finite volume method (FVM). Assuming the HTF is completely mixed in the storage tank, lumped tank model is employed to obtain the storage HTF temperature. The collector field outlet temperature is imposed as a boundary condition to the lumped tank model as follows:

$$V_{tank} \rho c_p \frac{dT_{tank}}{dt} = \dot{m} c_p (T_{col,out} - T_{col,in}) - q_{loss,tank} - q_{load} \quad (\text{eq. 7})$$

where  $V_{tank}$  is the storage tank volume,  $T_{tank}$  is the storage HTF temperature,  $\dot{m}$  is the mass flow rate of HTF through the receiver pipe of PTC,  $T_{col,in}$  and  $T_{col,out}$  are collector inlet and outlet temperatures, respectively.  $q_{loss,tank}$  is the heat loss to the environment from the storage tank, it is calculated in a similar manner to eq. 6.  $q_{load}$  is the process heat load on the solar thermal system that is used to boil olive mill waste water. Then, the flow rate of waste-water that can be boiled using solar heat can be calculated as:

$$\dot{m}_w = \frac{q_{load}}{h_{fg}} \quad (\text{eq. 8})$$

where  $\dot{m}_w$  is the maximum flow rate of olive mill waste-water that can be boiled using solar heat and  $h_{fg}$  is

the latent heat of boiling of water under vacuum pressure. Although  $h_{fg}$  slightly increases with decreasing pressure, vacuuming the drying chamber is still beneficial due to the lower temperature requirement of the drying process. In addition, reduced boiling temperature results in increased temperature difference which enhances heat transfer from HTF to olive mill wastewater.

For ETC solar field we considered a solar plant of 514 m<sup>2</sup> composed of 150 collectors, the solar plant uses pressurized water as the HTF. The empirical technical data about optical efficiency ( $a_0$ ) and heat losses of 1<sup>st</sup> and 2<sup>nd</sup> order ( $c_1, c_2$ ) of the commercial ETC used, are presented in the Table 2(Bolognese *et al.*, 2020)

Tab. 2: Coefficients of efficiency and heat losses

$a_0(W/m^2)$	$c_1(W/m^2K)$	$c_2(W/m^2K^2)$
0.718	0.974	0.005

Moreover, the overall efficiency  $\eta$  depends on the longitudinal and transversal Incidence Angle Modifiers ( $K_l, K_t$ ) which are necessary to calculate the effective efficiency  $\eta$ .

$$\eta = K_l K_t a_0 - c_1 \frac{(T_* - T_{ext})}{GHI} - c_2 \frac{(T_* - T_{ext})^2}{GHI} \quad (\text{eq. 6})$$

Here  $T_*$  is the average temperature of solar collectors ( $T_* = \frac{T_{in} + T_{out}}{2}$ ) and  $T_{ext}$  is the environmental temperature. In order to analyse the dynamic transient behaviour of a solar field composed of ETC the commercial dynamic simulation software Dymola - Dassault Systems (Dassault Systèmes, 2017)with the *Thermocycle* library (Desideri *et al.*, 2018) were used. In the dynamic simulation, the mass flow rate and recirculation loop are controlled by two proportional integrative (PI) controllers using the outlet hot water tank temperature as measurement point and the temperature of 90 °C as the set point. If the temperature does not reach 90 °C, the flow rate decreases while the recirculation valve opens. The configuration of the solar field consists of 15 solar collectors in parallel and 10 solar collectors in series.

PVGIS (*PVGIS*) has been used as the source for the solar radiation data from a Typical Meteorological Year (TMY). In particular, the Global Horizontal Irradiation (GHI) has been taken for 21-23 June, in Rome (Lat: 41.895°, Long: 12.485°).

### 3. Modelling results

To understand the technical feasibility of a solar dryer, two solar plants with two kinds of solar collector were modelled:

- i) Vacuum Solar dryer with ETC collector and water as the working fluid
- ii) Vacuum Solar dryer with PTC collector and water as the working fluid

The performance of solar dryers was calculated for 21-23 June considering Rome as the location of the plant. The area of collectors for both the solar fields are similar and limited around 500m<sup>2</sup>. The collector areas are slightly underpowered, (in particular, ETC) to understand the impact of the vacuum dryer technology. For the ETC solar field, we considered a tank with a storage capacity of 1 m<sup>3</sup> while for PTC solar field, a storage tank of 6 m<sup>3</sup> is assumed. Tab reports a summary of the main characteristic of the solar plant structure used to obtain the different performances in the modelling of the solar vacuum dryer.

Tab. 3: Summary of the main characteristic of the solar plant structure used to obtain the best performance in the modelling of the solar vacuum dryer.

	Total Collector Area [m <sup>2</sup> ]	N Collector Series / Parallel	Storage Capacity [m <sup>3</sup> ]	Temp. Range [°C]	Avg. working hours per day		
					[1000 mbar / No vacuum]	[500 mbar]	[200 mbar]
ETC	514	10/15	1	90-60	0	3.94	9.08
PTC	480	12/10	6	80-120	9.82	10.97	12.29

Fig. 4 shows the temperature of the working fluid (red) and the temperature of water in the tank (blue). The days of the 21<sup>st</sup>-23<sup>rd</sup> of June were considered (72 hours) for the ETC solar field. We remark, as the energy source which turns the drying cycle is solar powered (therefore not stable during the day) the system should be adaptive to the power input; for instance, arranging the vacuum pressure inside the solar drying tank. For

instance, if there is a low power input to the system (temporarily cloudy), the vacuum pressure can be reduced to reduce the boiling temperature of the water, making it easier to dry the water sludge. Even if ETC solar field is underpowered (limited field area), thanks to the good efficiency of ETC, the maximum temperature reached at atmospheric pressure by the working fluid is relatively high 85°C; but not enough to obtain effective boiling of the water at ambient pressure (considering this solar dryer). While the estimated boiling temperatures at different vacuum pressures, 500mbar and 200mbar, are 81.5°C and 60.5°C, respectively (highlighted as horizontal lines in Fig. 4). Considering these boiling temperatures, we have estimated the average hours per day where the dryer is effectively fed by the solar field (see Tab).

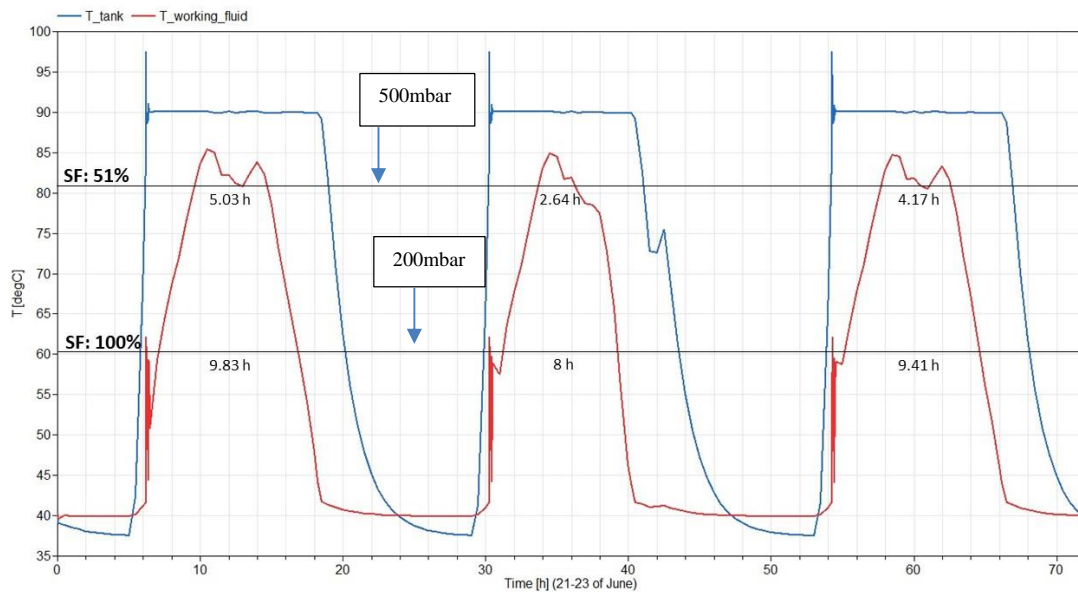


**Fig. 4:** Distributions of temperatures of Storage Tank and Working fluid are reported along 72 hours, from 21<sup>st</sup> to 23<sup>rd</sup> of June in Rome. Two black horizontal lines highlight the necessary temperatures to feed the solar dryer at 500 mbar or 200 mbar. The hours of actual feed of the solar dryer for the different vacuum conditions are also reported.

The ETC results show that with a pressure of 500 mbar, it is possible to cover the thermal energy demand of the drying processes for around 4 hours per day; while at 200 mbar, it covers more than 8 hours per day. If a more complex and expensive pumping system is employed, the pressure can be furtherly decreased to 100 mbar, and the ETC's can cover the energy demand for more than 10 hours. The simulation of the PTC solar field using the same conditions of the solar radiation revealed that at atmospheric pressure it is possible to cover the thermal energy demand of the drying processes for around 9.82 hours per day; (81.8% solar fraction); while at the pressure (inside the solar dryer) of 500 mbar, is possible to reach a solar fraction of 91.4% for 10.97 hours on an average day in June. By simulation, it is also found that increasing the mass flow rate from 1.5 kg/s to 3.0 kg/s allows to decrease the heat losses and to increase the solar fraction from 89.7% to 91.4% (considering this solar dryer). As a summary, we observed that in the ETC solar field with limited gross area, without vacuum, it is not possible to dry the water sludges using this solar dryer, while it is possible for several hours using a vacuum pressure of 500 mbar (estimated solar fraction around 50%). For the PTC solar field, using this solar dryer, the solar fraction at ambient conditions is around 81.8% but with a vacuum pressure of 500mbar, it is possible to reach a value of 91.4 % (leads to a solar fraction increase of 12%). With both solar thermal technologies, ETC and PTC, it is possible to cover a solar fraction of 100% using a vacuum pressure of 200 mbar. The simulation results show that using a relatively small depression in the solar dryer pressure (500-200 mbar) allows an increase in both kinds of systems, ETC and PTC. We remark that at this range of vacuum pressure (rough vacuum) the vacuum system does not require expensive, sophisticated pumps or sensors such as turbomolecular pumps or thermionic sensors. Therefore, the cost of a solar vacuum dryer could be quite affordable for industrial applications

## 4. Acknowledgements

This research work was implemented in the framework of the EU H2020 LCE-33-2016 (RIA) project INSHIP Integrating National Research Agendas on Solar Heat for Industrial Processes, GA 731287, duration 01.01.2017 – 31.12.2020, <https://www.inship.eu/>

## 5. References

Bal, L. M., Satya, S. and Naik, S. N. (2010) ‘Solar dryer with thermal energy storage systems for drying agricultural food products : A review Solar dryer with thermal energy storage systems for drying agricultural food products : A review’, *Renewable and Sustainable Energy Reviews*. Elsevier Ltd, 14(8), pp. 2298–2314. doi: 10.1016/j.rser.2010.04.014.

Bekkioui, N. *et al.* (2011) ‘Solar drying of pine lumber: Verification of a mathematical model’, *Maderas. Ciencia y tecnología*, 13(1), pp. 29–40. doi: 10.4067/S0718-221X2011000100003.

Bennamoun, L. (2012) ‘Solar drying of wastewater sludge: A review’, *Renewable and Sustainable Energy Reviews*, pp. 1061–1073. doi: 10.1016/j.rser.2011.10.005.

Bolognese, M. *et al.* (2020) ‘Modeling study for low-carbon industrial processes integrating solar thermal technologies . A case study in the Italian Alps : The Felicetti Pasta Factory’, *Solar Energy*. Elsevier Ltd, 208(August), pp. 548–558. doi: 10.1016/j.solener.2020.07.091.

Dassault Systèmes (2017) *Dymola Systems Engineering*. Available at: <https://www.3ds.com>.

Dermeche, S. *et al.* (2013) ‘Olive mill wastes: Biochemical characterizations and valorization strategies’, *Process Biochemistry*. Elsevier Ltd, 48(10), pp. 1532–1552. doi: 10.1016/j.procbio.2013.07.010.

Desideri, A. *et al.* (2018) ‘Steady-state and dynamic validation of a parabolic trough collector model using the ThermoCycle Modelica library’, *Solar Energy*, 174, pp. 866–877. doi: 10.1016/j.solener.2018.08.026.

Encinar, J. M. *et al.* (2008) ‘Pyrolysis and catalytic steam gasification of olive oil waste in two stages’, *Renewable Energy and Power Quality Journal*, 1(6), pp. 697–702. doi: 10.24084/repqj06.415.

Fuller, R. J. (2002) ‘NATURAL CONVECTION SOLAR DRYER WITH BIOMASS BACK-UP HEATER’, 72(1), pp. 75–83.

Goh, L. J. *et al.* (2011) ‘Review of heat pump systems for drying application’, 15, pp. 4788–4796. doi: 10.1016/j.rser.2011.07.072.

Gouveia, L. *et al.* (2016) ‘Microalgae biomass production using wastewater: Treatment and costs. Scale-up considerations.’, *Algal Research*. Elsevier B.V., 16(June), pp. 167–176. doi: 10.1016/j.algal.2016.03.010.

Hisan, S. *et al.* (no date) ‘Solar Process Heat in Industrial Systems- A Global Review’, pp. 1–20.

Prakash, O. and Kumar, A. (2014) ‘Solar greenhouse drying: A review’, *Renewable and Sustainable Energy Reviews*. doi: 10.1016/j.rser.2013.08.084.

PVGIS (2020). Available at: <https://ec.europa.eu/jrc/en/pvgis> (Accessed: 31 May 2020).

Villagracia, A. R. C. *et al.* (2016) ‘Microwave drying characteristics of microalgae (*Chlorella vulgaris*) for biofuel production’, *Clean Technologies and Environmental Policy*. Springer Berlin Heidelberg, 18(8), pp. 2441–2451. doi: 10.1007/s10098-016-1169-0.

Wu, X. H. *et al.* (2010) ‘Dewatering and Drying in Mineral Processing Industry : Potential for Innovation’, *Drying Technology: An International Journal*, 28, pp. 834–842. doi: 10.1080/07373937.2010.490485.